Interdiffusion Behavior of Pt-Diffused γ+γ' Coatings on Ni-Based Superalloys

Y. Zhang and J. P. Stacy
Department of Mechanical Engineering, Box 5014
Tennessee Technological University, Cookeville, TN 38505-0001
E-mail: yzhang@tntech.edu; Tel.: (931) 372-3265; Fax: (931) 372-6345

B.A. Pint and J.A. Haynes
Metals and Ceramics Division
Oak Ridge National Laboratory, Oak Ridge, TN 37831-6156
E-mail: pintb@ornl.gov; Tel.: (865) 576-2897; Fax: (865) 241-0215

B.T. Hazel and B.A. Nagaraj
GE Aviation, Cincinnati, OH 45215-6301

ABSTRACT

Platinum-diffused γ+γ' coatings (~20 at.% Al, ~22 at.% Pt) were synthesized on René 142 and René N5 Ni-based superalloys by electroplating the substrates with ~7 μm of Pt, followed by an annealing treatment in vacuum at 1175°C. In order to study the compositional and microstructural evolution of these coatings at elevated temperatures, interdiffusion experiments were carried out on coated specimens in the temperature range of 900-1050°C for various durations. Composition profiles of the alloying elements in the γ+γ' coatings before and after diffusion experiments were determined by electron probe microanalysis. Although the change of the Al content in the coatings was minimal under these interdiffusion conditions, the decrease of the Pt content and increase of the diffusion depth of Pt into the substrate alloys was significant. A preliminary diffusion model was used to estimate the Pt penetration depth after diffusion.

INTRODUCTION

The constant demand for increased operating temperatures in gas turbine engines has been the driving force for development of more reliable thermal barrier coating (TBC) systems to protect Ni-based superalloys.[1] Single-phase β-(Ni,Pt)Al [2] represents a class of bond coatings for the TBCs deposited by electron beam-physical vapor deposition (EB-PVD). Failure of EB-PVD TBCs is often associated with spallation of the Al_2O_3 scale along the scale-bond coat interface.[3] In service, due to the formation of Al_2O_3 scales and interdiffusion with superalloy substrates, depletion of Al occurs from the bond coating that leads to transformations of the as-deposited β phase to more Ni-rich phases such as martensite and γ'-Ni_3Al.[4,5] The volume changes associated with these phase transformations could contribute to rumpling at the bond coat surface and affect the ability of the bond coat to maintain an adherent Al_2O_3 scale.[6-8] Studies by Gleeson et al. [9-11] demonstrated that the γ+γ'-based coatings consisting of Ni-20Al-22Pt-7Co-7Cr-0.7Hf (at.%) could form adherent Al_2O_3 scales with significantly reduced rumpling during thermal cycling. Our recent work [12-15] investigated the issues related to synthesis and oxidation performance of the γ+γ' coatings; the results suggested that the oxidation behavior of the γ+γ'-type coatings was very sensitive to the superalloy substrate composition. The effect of Pt on interdiffusion of γ+γ'-based alloys at 1150°C was studied by Hayashi et al. [16] using diffusion couples comprised of a γ+γ' Ni-Al-Pt alloy mated to Ni-based superalloys. The present study focused on the interdiffusion behavior of Pt-diffused γ+γ' coatings on Ni-based superalloys in the temperature range of 900-1050°C. The lower temperature end was included to represent potential applications in land-base gas turbines.[17]

EXPERIMENTAL PROCEDURE

Two types of Ni-based superalloys were used as substrates, the directionally-solidified (DS) alloy René 142 (PCC Airfoils) and the single-crystal Y-free René N5 (Howmet Corporation). The DS alloys are less expensive than single crystals, especially when considered for large-sized components in land-base turbine engines. All compositions are given in at.%, unless noted otherwise. The composition of the 142 alloy was Ni-13.4Al-7.7Cr-11.9Co-2.1Ta-1.6W-0.9Re-0.9Mo (at.%), with 4451Hf-38S-5513C (ppma). The composition of the N5 was Ni-13.7Al-8.0Cr-7.1Co-2.2Ta-1.6W-0.9Re-0.9Mo, with 47Hf-6S-2490C (ppma). Superalloy specimens (16.5mm in diameter x 1.5mm) were electroplated with ~7 μm Pt, followed by a diffusion treatment of 2h in vacuum at 1175°C to form the γ+γ' coating.[12,13] Prior to electroplating, the substrates were prepared by grit blasting using #220 Al_2O_3 grit and ultrasonically cleaned in acetone. Each of the coated coupons was sectioned into four pieces. One quarter of the specimen was used for characterization of the as-coated condition, and the other three pieces were used in the interdiffusion experiments. The specimens were ultrasonically cleaned in acetone and methanol before they were sealed in an Ar-filled quartz capsule. The diffusion annealing was carried out in the temperature range of 900-1050°C; the conditions are given in Table I. After the experiments, the quartz capsule was removed from the furnace and air cooled to room temperature. Following the diffusion experiments, the specimens were coated with Cu prior to sectioning for cross-sectional observation by scanning electron microscopy (SEM, FEI Quanta 200) equipped with energy dispersive spectroscopy (EDS). The concentration profiles of alloying elements in the coating samples were determined by electron probe microanalysis (EPMA, JEOL 8200 Electron Superprobe) using pure metal standards.

Table I. Measured and estimated diffusion depths of Pt after high temperature exposures.

Experimental Conditions			Pt Diffusion Depth (μm)		
Substrate Alloy	Temperature (°C)	Time (h)	Measured Depth	Calculated Depth	
				Using $D_{Pt(\gamma)}$ [24]	Using $D_{Pt(\gamma')}$ [25]
142	As-coated		40	—	—
N5	As-coated		38	—	—
N5	900 [A]	1000	44	50	45
142	1000 [A]	1000	79	78	65
142	1050 [A]	1000	107	105	84
N5	1050 [A]	1000	98	103	82
142	1100 [B]	300, 1h cycles [12]	94	87	71
N5	1150 [B]	1000, 1h cycles [20]	205	200	160
N5	900 [C]	40,000†	N/A	113	81
N5	1050 [C]	15,000†	N/A	288	209

[A]—Annealed in Ar

[B]—Oxidized in air

[C]—Assumed exposure time for land-base gas turbine systems

RESULTS AND DISCUSSION

3.1. As-Synthesized γ+γ′ Coatings

Figure 1 shows the concentration profiles of major alloying elements (Ni, Pt, Al, Cr and Co) in an as-fabricated coating on N5 (the corresponding cross-sectional image is shown in Fig. 2a). The γ+γ'

coating was formed by inward diffusion of Pt and outward diffusion of alloying elements in the superalloy substrate during the post-plating annealing treatment.[18] The average Al and Pt contents in the outer coating layer, which was ~16 μm thick and consisted primarily of γ', were ~20 and 22%, respectively. Cr and Co were present at levels of ~2 and 4%, respectively. The interdiffusion distance, determined as the penetration depth of Pt to a point where Pt < 0.5%, was ~38 μm. Although not included in Fig. 1, there also was incorporation of refractory elements from the superalloy into the γ+γ' coating, with an average level of 1.4Ta, 1.0W, 0.8Re, and 0.8Mo. Moreover, in agreement with the results of Gleeson and Hayashi's diffusion couple experiments,[9,16] Al enrichment in the coating was evident in Fig. 1, indicating that there was uphill diffusion of Al from the superalloy substrate into the Pt-containing γ+γ' coating.

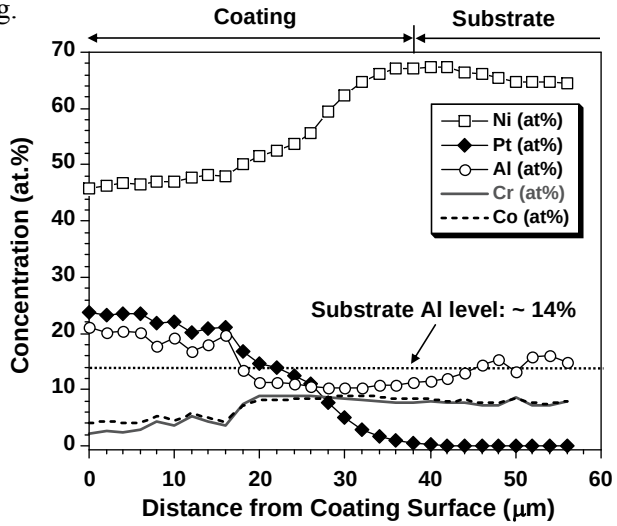

Fig 1. EPMA concentration profiles of major alloying elements in the as-coated γ+γ' coating on René N5.

3.2. Interdiffusion Experiments at Different Temperatures

The cross sections of the γ+γ' coating on N5 before and after 1000h diffusion annealing at 900°C are shown in Figs. 2a-b. The black particles in the outer portion of the coating were from the grit-blasting process. In the as-coated condition, two distinct phases were present in the coating, Fig. 2a. The majority phase was Al-enriched γ' (with light-contrast on the BSE image), and the darker phase was γ with lower Al. While the two-phase microstructure was maintained in the coating after diffusion, the γ' phase in the inner part of the coating became more agglomerated. In addition, small white precipitates (arrows in Fig. 2b) were formed in the coating after 1000h at 900°C. These precipitates were rich in Re and W, suggesting that they were some type of topologically close-packed (TCP) phases.[19] However, no such precipitates were observed in a γ+γ'-coated N5 sample after 1000, 1h cyclic oxidation at 1150°C.[20] Karunaratne et al. [21] studied the microstructural stability of an uncoated single-crystal Ni-based superalloy upon exposures in the temperature range of 700-1150°C. Their results showed that annealing at 800-1100°C caused TCP precipitation, whereas no such precipitates were formed after 3600h at 700°C or after 500h at 1150°C.[21] Similar temperature dependence may exist for the TCP formation in the γ+γ' coating on N5. Furthermore, interdiffusion between the Pt-enriched coating and the single-crystal superalloy somehow promoted the TCP precipitation because no precipitates could be found deep in the substrate.

The changes in the Al and Pt concentration profiles of the coating on N5 are illustrated in Fig. 3. The Al level remained ~20% in the coating after 1000h diffusion at 900°C, whereas the Pt content at the coating surface decreased from ~24 to 18%. The penetration depth of Pt increased slightly compared to the as-formed coating.

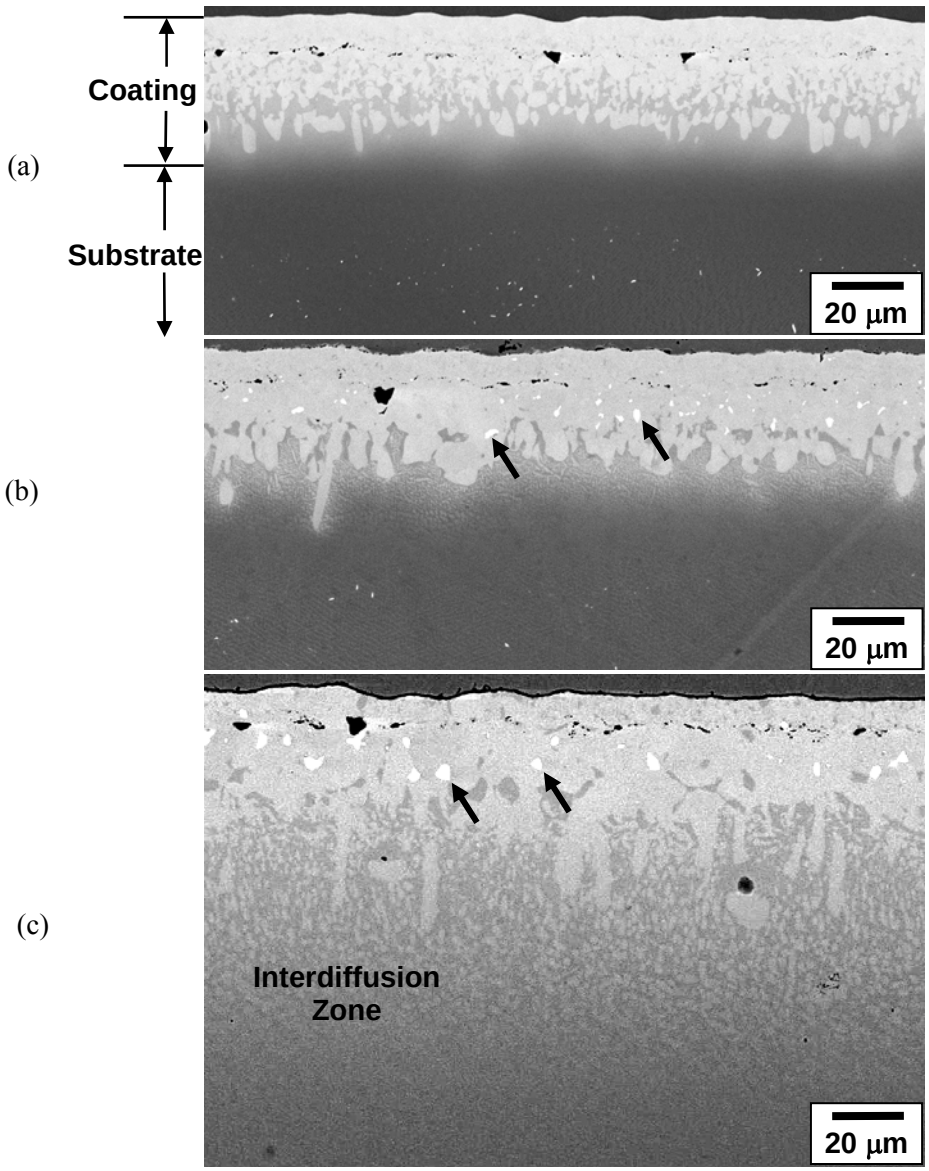

Fig. 2. BSE cross-sectional images of the γ+γ' coatings on René N5: (a) as-coated condition, (b) after 1000h interdiffusion at 900°C, and (c) after 1000h at 1050°C.

Figures 4a and 4b show the cross sections of the γ+γ'-coated 142 before and after annealing for 1000h at 1000°C. Numerous voids were seen in the substrate adjacent to the coating even in the as-synthesized condition, and the size of the voids increased after diffusion. When the diffusion fluxes of different elements across the coating/substrate interface were not balanced, Kirkendall voids could form if sufficient vacancy sinks were not available. Yet, no such voids were present in the γ+γ'-coated N5, Fig. 2. Purvis and Warnes [22] observed Kirkendall porosity in Pt-plated pure Ni after 2-6h annealing at 950 and 1080°C, as a result of faster diffusion of Ni than Pt. For Pt-coated superalloys, since all alloying elements (including the refractory elements) displayed significant diffusional motion,[22] the diffusion fluxes could differ drastically from the binary system. As compared to the single-crystal N5, the DS alloy 142 exhibited columnar grains, which could increase the diffusion flow of the alloying elements via grain boundary diffusion. Also, the sites available as vacancy sinks may alter. More work is needed to clarify the cause for the different responses regarding void formation in γ+γ'-coated 142 and N5.

Regardless of the substrate alloys, comparison of Figs. 2b and 4b reveals that more interdiffusion occurred at 1000°C, where the diffusion depth was nearly doubled (from 40 to 79 μm for coated 142) after 1000h (Table I). A noticeable interdiffusion zone was formed underneath the coating, consisting of small precipitates of Pt-containing γ' phase in a γ matrix. Unlike the coating on N5, no TCP precipitates were formed in the γ+γ' coating on 142 after diffusion. Even though the two alloys had similar chemical compositions and contained essentially the same levels of refractory metals, in contrast to single crystals, the refractory metals in the DS alloys were more tied up in the form of stable carbides,[23] which could reduce the TCP precipitation in the coating.

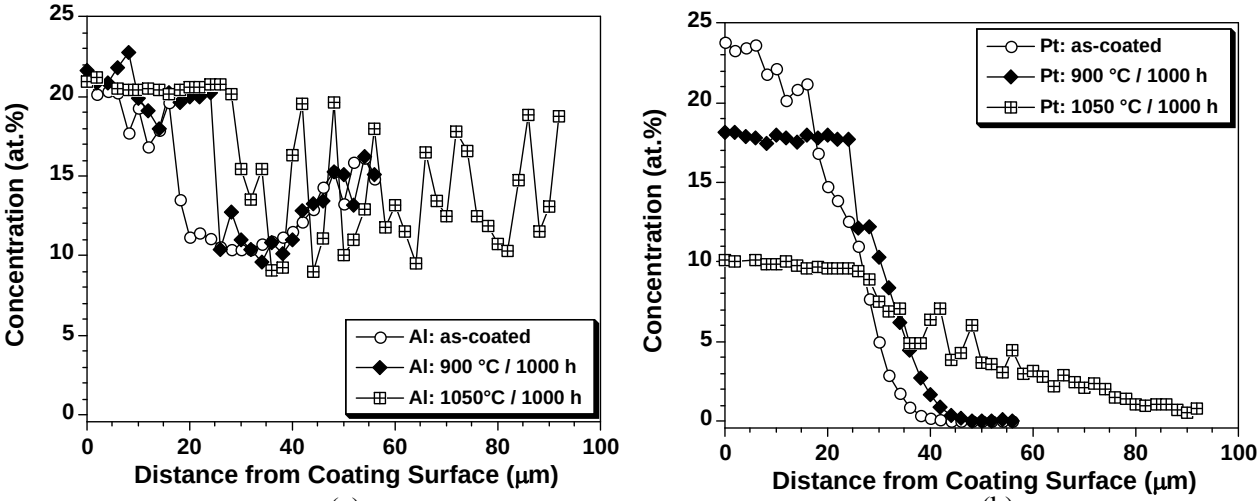

(a) (b)

Fig. 3. EPMA concentration profiles of Al and Pt in the γ+γ' coating before and after 1000h diffusion annealing at 900 and 1050°C: (a) Al profiles and (b) Pt profiles.

When the temperature was further increased to 1050°C, Pt backdiffusion occurred to a depth of approximately 100-110 μm after 1000h in both coated alloys, Figs. 2c and 4c. The Pt-enriched γ' precipitates in the interdiffusion zone were more evident. The size of the TCP phases in the coating on N5 also increased. Again, no TCP precipitates were observed in the coated 142. Note that oxidation occurred for the coating on 142 (as pointed out by the arrow in Fig. 4c), as a result of cracking of the quartz capsule during the experiment. Compared to Fig. 2c, Fig. 4c shows that the consumption of Al by oxidation reduced the amount of γ' phase near the coating surface. The external oxidation did not seem to affect Pt diffusion significantly, where the diffusion depth of Pt was only slightly greater than that on N5. It is worth mentioning that the non-uniform coating/substrate interface caused by the presence of the blocky γ' phases (Figs. 2b-c and 4b-c) could contribute to variations in Pt penetration depths on the levels of several microns, depending on where the EPMA profiles were taken. As shown in Fig. 3a, the Al level remained at ~20% after 1000h at 1050°C in the coating on N5. The Pt content at the coating surface, however, decreased from ~24 to 10%, Fig. 3b. These results demonstrated that the Al uphill diffusion was still effective after 1000h at 1050°C. Both Al and Pt profiles became more uniform in the outer coating layer, while large variations were observed in the interdiffusion zone, particularly for the Al profile, due to the presence of the Pt-containing γ' precipitates. The disruption of the original fine γ/γ' microstructure in this substrate region may affect the alloy creep strength, particularly for thin-walled airfoils.[23]

3.3. Estimation of Pt Penetration Depth

The penetration depth of Pt was estimated using a very preliminary diffusion model. A simple version of the diffusion couple representing the current coating system was taken to be γ+γ' (Ni-20Al-

22Pt) / γ+γ' (Ni-14Al). However, both the coating and substrate contained a variety of additional alloying elements, resulting in a complicated, multicomponent, multiphase diffusion system. Interdiffusion in a multicomponent system often is affected by chemical interactions among various components. In addition, as indicated by the Pt profiles in Fig. 3b, the present γ+γ'-coated superalloys did not exhibit fixed terminal compositions as in traditional infinite solid diffusion couples. During the initial post-plating annealing treatment (2h at 1175°C), the γ+γ' coating may be approximated as a thin film at the end of a semi-infinite bar. Even so, it cannot be considered to be a classic thin film diffusion case because of the presence of the two phases in the coating. Therefore, with regard to the increase in Pt penetration depth (Δx) after the diffusion experiments, only a semi-quantitative estimation was achieved, using the equation $\Delta x = 2\sqrt{Dt}$ (where t is the exposure time and D is the diffusion coefficient of Pt).

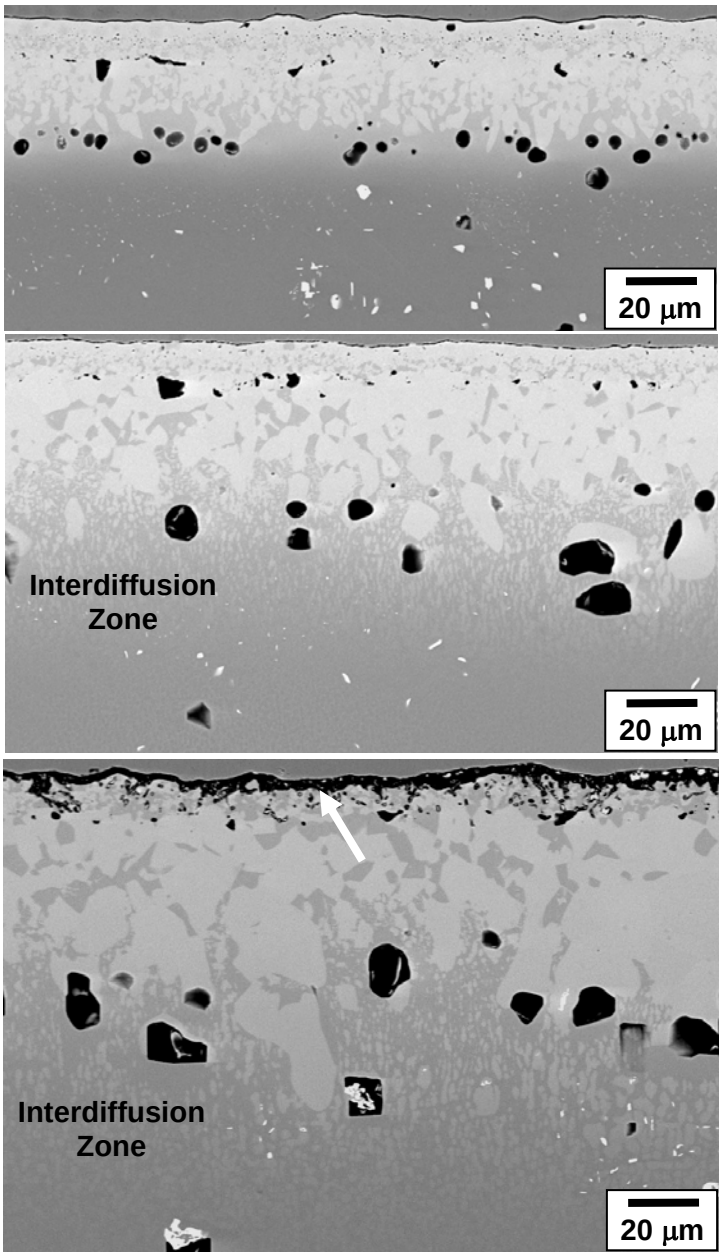

Fig. 4. BSE cross-sectional images of the γ+γ' coatings on René 142: (a) as-coated condition, (b) after 1000h interdiffusion at 1000°C, and (c) after 1000h at 1050°C.

In the literature, the diffusion coefficient of Pt in γ-Ni and γ'-Ni_3Al can be found only for dilute Pt concentrations:[24,25]

$$D_{Pt}(\gamma)\,(m^2 s^{-1}) = 9.2\times10^{-5}\exp(-291.2\ \ kJ\,mol^{-1}/RT),\ [24]\ \text{in } \gamma\text{-Ni, Pt} = \sim 3.2\ \% \qquad [1]$$

$$D_{Pt}(\gamma')\,(m^2 s^{-1}) = 7.8\times10^{-4}\exp(-323\ \ kJ\,mol^{-1}/RT),\ [25]\ \text{in } \gamma'\text{-Ni}_3\text{Al, Pt} = \sim 2.1\% \qquad [2]$$

The Pt levels in the current γ+γ' coatings, however, were in the range of 10 to 23%, much higher than a dilute concentration. Also, with the increased Pt levels, the Pt diffusivities can be concentration dependent. Due to the lack of such diffusion data, the D_{Pt} values derived from the above expressions for various temperatures were used in the present calculation, and the estimated Pt diffusion depths are summarized in Table I. Two γ+γ' coating samples after cyclic oxidation tests at 1100 [12] and 1150°C [20] are included for comparison.

Despite the simplified estimation method, the penetration depth of Pt measured from the concentration profile was quite close to the values calculated using $D_{Pt(\gamma)}$ and $D_{Pt(\gamma')}$. It also appeared that when the interdiffusion was limited, such as after 1000h at 900°C, the estimated depth using the Pt diffusivity in γ' was closer to the measured depth. When more interdiffusion occurred at higher exposure temperatures, e.g. 1000-1150°C, the estimation using $D_{Pt(\gamma)}$ gave a better fit. These results agreed well with the cross-sectional observations that the coating still contained a high percentage of γ' after 900°C diffusion (Fig. 2b), whereas the interdiffusion zones consisting of the fine Pt-enriched γ' precipitates in a γ matrix became significantly larger at temperatures ≥ 1000°C (Figs. 2c, 4b and 4c). For the specimen after oxidation in air for 1000, 1h cycles at 1150°C,[20] the Pt penetration depth increased from ~40 μm to ~205 μm.

In contrast to aircraft engines, the operating time of land-based gas turbine systems can be as 25,000h or longer between overhauls and refurbishment.[17] The simple diffusion model also was applied to predict the Pt penetration depth after prolonged exposure time, such as 40,000h at 900°C and 15,000h at 1050°C, Table I. If the more conservative values are taken into account, i.e., using $D_{Pt(\gamma)}$, the results indicated that for an initial coating of ~40μm thick, Pt may diffuse in a distance of ~113μm after 40,000h at 900°C. At 1050°C, the Pt penetration distance can be ~288μm after 15,000h. As expected in any diffusion processes, the temperature plays a rather critical role. As suggested by Gleeson and Hayashi,[9,16] a sufficient Pt level (e.g., > 15%) is necessary to cause uphill Al diffusion in the γ+γ' Ni-Al-Pt alloys or coatings. Significant loss of Pt to the substrate via interdiffusion may increase the Al activity in the γ+γ' coating to a level that uphill diffusion of Al becomes ineffective and Al replenishment may cease. Insufficient Pt in the coating could also diminish the beneficial effect of Pt on coating oxidation resistance.[9] A more sophisticated model that enables to predict the Pt profiles of the γ+γ' coatings is undoubtedly needed. Utilizing diffusion couples with compositions representative of the present coated alloys, "effective interdiffusion coefficients" could be determined for each alloying element using an approach developed by Dayananda et al.[26,27] The effective interdiffusion coefficients may then be employed to more accurately model Pt backdiffusion in a multicomponent multiphase assembly.

CONCLUSIONS

The interdiffusion behavior of Pt-diffused γ+γ' coatings was investigated at 900-1050°C. While the change in the Al content and diffusion-induced microstructural evolution were insignificant in coatings on superalloy N5 after 1000h at 900°C, a decrease of the Pt content at the coating surface from 24 to 18% was observed, which further decreased to 10% if the diffusion temperature was raised to 1050°C. After 1000h interdiffusion at 1000°C, the Pt diffused into a 142 superalloy substrate to a depth that doubled the original 40-μm coating thickness, while at 1050°C the diffusion depth of Pt was ~100-

110 μm for both 142 and N5. However, under all these diffusion conditions, uphill Al diffusion was retained, which was reflected by the minimal change in the Al content in the outer coating layer. The Pt penetration depth after interdiffusion estimated using a preliminary diffusion model showed reasonable agreement with the experimental data.

ACKNOWLEDGEMENTS

The authors acknowledge L.R. Walker at Oak Ridge National Laboratory (ORNL) and L.R. Liu at Tennessee Technological University (TTU) for assisting with the experimental work, and I.G. Wright and T.M. Besmann at ORNL for reviewing the manuscript. This material is based upon work supported by the National Science Foundation-GOALI Program under Grant No. 0504566. Additional support is from the U.S. Department of Energy, Fossil Energy Advanced Materials Research Program, under contract DE-AC05-00OR22725 with UT-Battelle LLC and subcontract 4000032193 with TTU.

REFERENCES

1. G.W. Goward, Surf. Coat. Technol., 108-109 (1998) 73.
2. I.G. Wright and B.A. Pint, Proc. IMechE, J. Power and Energy, 219 (2005) 101.
3. I.T. Spitsberg, D.R. Mumm, and A.G. Evans, Mater. Sci. Eng., 394 (2005) 176.
4. Y. Zhang, J.A. Haynes, B.A. Pint, I.G. Wright, and W.Y. Lee, Surf. Coat. Technol., 163-164 (2003) 19.
5. M.W. Chen, R.T. Ott, T.C. Hufnagel, P.K. Wright, and K.J. Hemker, Surf. Coat. Technol., 163-164 (2003) 25.
6. V.K. Tolpygo and D.R. Clarke, Acta Mater., 48 (2000) 3283.
7. D.R. Mumm, A.G. Evans, and I.T. Spitsberg, Acta Mater., 49 (2001) 2329.
8. B.A. Pint, S.A. Speakman, C.J. Rawn, and Y. Zhang, JOM, Jan. (2006) 47.
9. B. Gleeson, W. Wang, S. Hayashi, and D. Sordelet, Mater. Sci. Forum, 461-464 (2004) 213.
10. V. Deodeshmukh, N. Mu, B. Li, B. Gleeson, Surf. Coat. Technol., 201 (2006) 3836.
11. T. Izumi, N. Mu, L. Zhang, and B. Gleeson, Surf. Coat. Technol., 202 (2007) 628.
12. Y. Zhang, B.A. Pint, J.A. Haynes, I.G. Wright, Surf. Coat. Technol., 200 (2005) 1259.
13. Y. Zhang, D.A. Ballard, J.P. Stacy, B.A. Pint, J.A. Hyanes, Surf. Coat. Technol., 201 (2006) 3857.
14. J.P. Stacy, Y. Zhang, B.A. Pint, J.A. Haynes, B.T. Hazel, and B.A. Nagaraj, Surf. Coat. Technol., 201 (2007) 632.
15. J.A. Haynes, B.A. Pint, Y. Zhang, and I.G. Wright, Surf. Coat. Technol., 201 (2007) 730.
16. S. Hayashi, W. Wang, D.J. Sordelet, and B. Gleeson, Metall. Mater. Trans., 36A (2005) 1769.
17. W.P. Parks, E.E. Hoffman, W.Y. Lee, and I.G. Wright, J. Thermal Spray Technol., 6 (1997) 187.
18. H.M. Tawancy, A.I. Mohamed, N.M. Abbas, R.E. Jones, and D.S. Rickerby, J. Mater. Sci., 38 (2003) 3797.
19. R. Darolia, D. F. Lahrman R. D. Field, and R. Sisson, in Superalloys 1988, ed. by S. Reichman, D. N. Duhl, G. Maurer, S. Antolovich, and C. Lund, (TMS, 1988), p.255.
20. J.A. Haynes, B.A. Pint, Y. Zhang, and I.G. Wright, submitted to Surf. Coat. Technol., 2008.
21. M.S.A. Karunaratne, C.M.F. Rae, and R.C. Reed, Metall. Mater. Trans., 32A (2001) 2409.
22. A.L. Purvis and B.M. Warnes, Surf. Coat. Technol., 133-134 (2000) 23.
23. B.A. Pint, J.A. Haynes, K.L. More, J.H. Schneibel, Y. Zhang, and I.G. Wright, submitted to Superalloys 2008, ed. by K.A. Green et al., (TMS, 2008).
24. M.S.A. Karunaratne and R.C. Reed, Acta Mater., 51 (2003) 2905.
25. Y. Minamino, H. Yoshida, S.B. Jung, K. Hirao, and T. Yamane, Defect Diff. Forum, 143-147 (1997) 257.
26. M.A. Dayananda and D.A. Behnke, Scripta Metall. Mater., 25 (1991) 2187.
27. M.A. Dayananda and Y.H. Sohn, Scripta Mater., 35 (1996) 683.